ICAS-80-4.1 CALCULATION OF THE FLOW FIELD AROUND ENGINE-WING-CONFIGURATIONS †

C. Haberland
Technical University of Berlin
Berlin, Germany

E. Göde
Sulzer Brothers Ltd.
Zürich, Switzerland

G. Sauer
Technical University of Berlin
Berlin, Germany

ABSTRACT

A panel method for the determination of the flow field around high bypass engines without limitations with respect to geometry, speed and mass flow rate is presented. Within this computation method any flow inside the engine contour causing an error in mass flow rate and pressure distribution has been eliminated by developing a mathematical model which represents the real physical flow by introducing a controlled distribution of singularities on the surface combined with suitable boundary conditions. Hence, this modified panel method allows to provide an arbitrary mass flow rate independent of the onset flow velocity satisfying the continuity of the inlet flow.

Checking the computation model for several axisymmetric inlets and engine contours, it turns out that the calculated velocities are physically accurate in the far field as well as near the engine and compare well with experimental results. To determine the spanwise and chordwise interference effects for typical engine positions the axisymmetric engine model as a first step is combined with an infinite unswept wing.

1. INTRODUCTION

Performance optimization of modern aircraft requires an optimal design of the engine inlet as well as a consideration of the interference effects between engine and aircraft leading to an optimal adaption of the propulsion group to the airframe. For high speed cruise as well as for low velocity a significant pressure recovery and an uniform flow in the compressor entrance plane are necessary since pressure losses and distortions of the intake flow caused by flow seperation with respect to engine incidence are resulting in engine power loss and additional mechanical stresses which can cause engine failure.

On the other hand the large diameters of modern high bypass engines and the related large mass flow rates lead to inlet and exhaust conditions which cannot be neglected, when determining lift and thrust of the total configuration. In particular the wing design is strongly influenced by the position and type of the engine. Disturbances of the engine operation, e.g. changes in the mass flow rate and interference of the exhaust jet have to be considered.

This engine airframe integration problem is important for V/STOL as well as for conventional aircraft: V/STOL-aircraft during transition flight develop secondary forces due to engine induction in the magnitude of the aerodynamic load. In comparison, conventional aircraft result in considerably smaller influences of the inlet flow and the jet induced flow due to the high onset flow velocities, but these can determine the economy of such aircraft.

In order to achieve an optimum aerodynamic design the theoretical determination of the engine induced flow is necessary, since not only an optimum of engine airframe integration can be found, but also the contour of the engine inlet can be adapted to the flight mission in an ideal way to avoid flow separation and to achieve a minimum total pressure loss in the inlet. To solve this problem the computation of the inviscid flow can already provide valuable results. Hence, a demand for a calculation method for determining the flow field around engine airframe configurations without limitations with respect to geometry, onset flow and mass flow rate becomes evident. Such a calculation method has to consider simultaneously the

- flow outside the engine (external flow)
- flow through the engine (internal flow)

to get an accurate representation of the inlet flow and the exhaust jet distribution. Here the mass flow rate of the engine must be selectable independent of onset flow conditions.

The first problem, the flow around an arbitrary body can be regarded as solved since there exist numerous numerical solutions based on the panel method firstly formulated by HESS and SMITH [1]. Because of the discretization of the body surface by means of this numerical singularity method limitations with respect to geometry can almost be omitted. The application of this method to flow calculations of conventional aircraft has shown that the calculated pressure distributions compare very well with experimental results obtained for subcritical flow [2].

However, the second problem, the calculation of the flow through a body causes much more difficulties resulting from the discretization of the surface. Since the kinematic flow condition can be satisfied in the collocation points only a (leakage) flow through the surface is possible leading to an error in mass flow rate and in pressure distribution on the inlet contour respectively.

Many calculations reveal that even special adapted panel methods only under certain assumptions are in a position to simulate the inlet contour as a streamline and to suppress leakage effects. An essential improvement is possible by the application of higher order panel methods with curved panels [3], but in this case a significantly higher computation effort is implicated [4,5]. However, developing a mathematical model with an adjusted choice and distribution of singularities one can suppress leakage effects without application of higher panel methods. In the presented paper this adaption is performed by combining vortex and doublet sheets on the fan shroud and taking source distributions on the center body. In addition, the engine model has to be completed by combining it with a jet model, since the results depend on the accurate simulation of the flow in the inlet but also at the jet boundary [6]. The jet induced flow can

† This research was supported by the German Science Foundation

be taken into account by introducing empirically determined entrainment velocities. Thus, it is possible to calculate the velocities induced in an arbitrary distance from the engine, and the calculation of interferences with the airframe becomes feasable.

2. NOTATIONS

$a_{i,j}$	influence coefficient (normally to the panel)
$b_{i,j}$	influence coefficient (tangentially to the panel)
c_p	pressure coefficient
d	diameter
$\vec{i},\vec{j},\vec{k}$	unit vectors of the axis x, y, z
i_v	virtual collocation point
$\dot{m}$	mass flow rate
$\vec{n}$	normal unit vector
q_j	source density in the point j
s	surface coordinate
$\vec{t}$	tangential unit vector
u,v	velocity components
x,y,z	coordinates
A	surface
A_i	inner area
D	engine diameter
C	chord length
C_E	fan shroud length
L_i	engine inlet length
N	number of singularity strengths
U_o	nozzle exit velocity
V_a	external flow velocity
V_E	entrance velocity
V_{tot}	total velocity
V_i	internal velocity
$V_{i,j}$	velocity in point i due to the panel j
V_{i_v}	velocity in the virtual collocation point
V_n	velocity normally to the panel
V_R	velocity in the rotor plane
V_t	velocity tangentially to the panel
V_∞	onset flow velocity
V_Z	jet entrainment velocity
X_o	chrodwise engine position
Z_o	vertical engine position
α,ρ	angles
γ	vortex strength
Δs	panel length
μ	doublet strength
σ	singularity strength

3. COMPUTATIONAL METHODS

3.1 Basis Panel Method

The singularity method is an approved tool for the calculation of the potential flow around arbitrary shaped bodies. The flow around the body is simulated by arranging sources, sinks or vortices on the surface or inside the body, depending on the flow problem, in such a way that the body contour becomes stream surface when it is superimposed with a translating onset flow. The flow inside the body is without physical signification when the boundary condition on the body surface is satisfied correctly.

As analytical methods fail for arbitrary body contours, numerical procedures have to be applied for the determination of resulting singularity distributions. Among several methods the panel method developed by HESS and SMITH [1] is exceptionally suitable because restrictions concerning the body geometry can be substantially neglected. The surface is divided into a number of plane field elements to which singularity sheets with constant strength are contributed (basic method), figure 1.

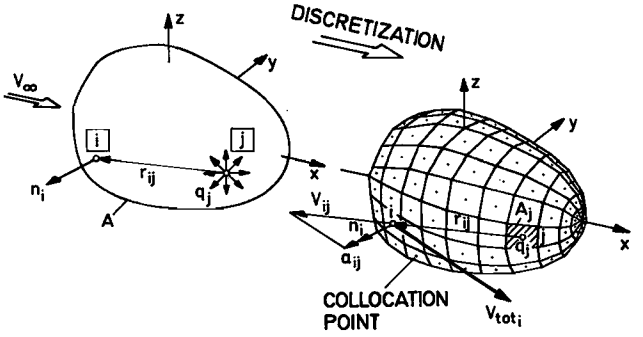

Figure 1. Source panel method

Thus the former continuous singularity distribution is substituted by finite source-, sink- or vortex elements and the kinematic flow condition has to be satisfied only in one point on each panel, the collocation point. The formulation of the flow condition for each collocation point yields a linear equation system for the determination of the unknown singularity intensities. Then the flow velocities in the entire flow field can be computed by summation of the contributions of each element and the onset flow.

In order to solve potential flow problems around non-lifting bodies it is known that the total velocity can be written as the sum of the onset velocity V_∞ and the disturbance velocity $\vec{v}$ induced by the body:

$$\vec{V}_{tot} = \vec{V}_\infty + \vec{v} \quad .$$

Hence, the potential problem is being reduced to the determination of the irrotational disturbance field

$$\vec{v} = - grad\ \varphi \quad ,$$

while the onset flow has not to satisfy a corresponding condition. The total potential of a body surface with continuously distributed sources

$$\varphi_{i,j} = \oint\!\!\oint_A \frac{q_j}{r_{i,j}}\, dA \quad , \tag{1}$$

and the kinematic flow condition leads to a Fredholm integral equation of the second kind

$$2\pi q_i - \oint\!\!\oint_A \frac{\partial}{\partial n}\left(\frac{1}{r_{i,j}}\right) \cdot q_j \, dA = -\vec{V}_\infty \cdot \vec{n}_i \quad . \tag{2}$$

Due to this equation the body contour may be considered to be a stream surface when the outward normal component of the disturbance velocity at an arbitrary point i of the surface just cancels the normal component of the onset flow. The disturbance field consists of the local term $2\pi q_i$ of the source in the field point itself and a "far field" term corresponding to the integral due the remaining set of sources on the contour.

This generally unsolvable integral equation can be approximated by discretization of the body surface. With the singularity distribution of constant strength on the panel (basic method) the kernel of the integral reduces to that term which is only dependent on the body geometry. Thus it is possible to solve the integral equation for each of these panels, and the kinematic flow condition is satisfied only in the collocation points. Substituting the surface integral by a sum and applying this boundary conditions, a set of linear equations results which coefficients consist of the outward normal velocity components corresponding to the kernel ot the integral. These are induced in each collocation point of all elements due to a source strength of unity.

The calculation of a lift generating flow requires the application of extended singularity models. For the calculation of the flow around wings it is not only sufficient, to satisfy the Kutta condition at the trailing edge, but the wake behind the wing has also to be taken into account. This can be done by defining an "inner plane" which is divided into panels like the surface itself [7]. A doublet distribution is used for these panels which intensity increases from zero at the leading edge of the wing to the maximum value at the trailing edge and remains constant along the wake.

Superposition of sources and doublets yields the total disturbance potential

$$\varphi_{i,j} = \oint\!\!\oint_A \frac{q_j}{r_{i,j}}\, dA + \iint_{A_i} \mu_j \frac{\partial}{\partial n}\left(\frac{1}{r_{i,j}}\right) dA_i \tag{3}$$

The first integral term in this equation represents the contribution of the sources on the wing surface, the second that of the doublets on the inner plane. Hence, the kinematic flow condition yields

$$\left(\frac{\partial \varphi}{\partial n}\right)_A = 2\pi q_i - \frac{\partial}{\partial n} \oint\!\!\oint_A \frac{1}{r_{i,j}} \cdot q_j \, dA$$

$$+ \frac{\partial}{\partial n} \oint\!\!\oint_{A_i} \frac{\partial}{\partial n}\left(\frac{1}{r_{i,j}}\right) \mu_j \, dA_i = -\vec{V}_\infty \cdot \vec{n}_i \tag{4}$$

Using constant source distributions and plane panels, inaccuracies in the calculation can occur which have two essential reasons:

- As a result of the plane panels the curved body contour is not approximated perfectly. Thus the collocation points do not lie on the body surface, and the induced velocity of the local term $2\pi q_i$ is wrong in magnitude and direction.
- As a consequence of applying a constant singularity sheet on each panel the contribution of the source density gradient to the tangential velocity component is neglected.

Accordingly, the "mathematical efficiency" of this model can be improved for bodies with non uniform surface curvature by increasing the number of panels and considering higher order terms, to get a better approximation of the exact continuous source distribution [8]. The error occuring in the calculation of the tangential velocity component is interpreted by HUNT and SEMPLE [9] as a consequence of the flow through the body surface between two collocation points. This leakage occurs because the boundary condition is satisfied in the collocation point on the panel only. The leakage even increases when additionally a pressure gradient is superposed on the body surface. That happens for instance for engine inlets with a prescribed mass flow rate. This influence grows with increasing divergence between the velocity in the rotor plane and the onset flow velocity. Thus the leakage error can be reduced if one succeeds in decreasing the difference of source densities between adjacent panel elements.

3.2 Panel Method for Engine Flow

Based on the method developed by KÜCHEMANN and WEBER [10] a number of numerical singularity methods have been developed. So HESS and SMITH [11] suggested the application of a source panel method for an idealized engine contour which consists of a real inlet and a cylindrical body, figure 2.

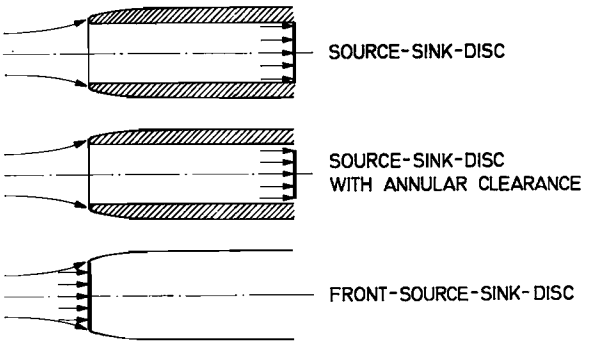

Figure 2. Earlier idealizations for inlet flow calculation

However, leakage losses occur along the inner inlet contour by using this method for real inlets with arbitrary mass flow rates. These errors can be avoided by positioning the rotor disc into the entrance cross section. But then it is only possible to compute the external flow field, the determination of the pressure distribution on the inner inlet contour is not possible.

This panel method can be improved by using additionally to the source distribution vortices on the inside or on the surface of the inlet. Thereby the sources generate the inlet contour while the variation of the mass flow rate is controlled by the vortices. For that either the trailing edge flow direction of the annular wing or the circulation on the section can be prescribed, figure 3.

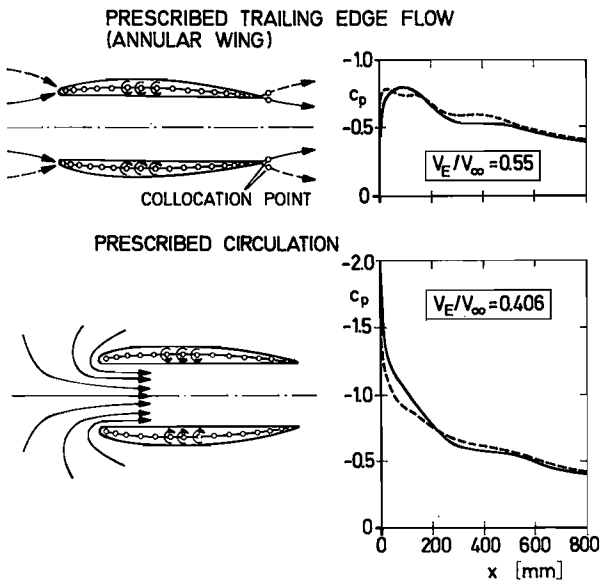

Figure 3. Vortex models for the calculation of the inlet NACA 1-70-50 (according to ZIMMER [12])

This method has been applied successfully for the calculation of engine inlets of conventional and V/STOL aircraft by STOCKMANN [13] whereas, however, the inlet contour had to be idealized in a suitable manner. Systems of vortices disposed on the chord of the investigated annular wing have been applied by ZIMMER [12], whilst GEISSLER [14] uses vortices also for a surface distribution and provides an additional circumferential variation of the singularity intensities by Fourier analysis, by which annular wings at angle of attack as well as the interference between several bodies can be investigated. TRULIN and IVERSEN [15] show that the application of a linearly varying vortex distribution on the contour substitutes an additional source and sink distribution on the section surface.

These models turn out to be problematic when the flow through the inlet is coupled with an engine jet because the prescription of a defined exit angle of the trailing edge flow is not compatible with the real exhaust jet distribution, empirically determinable. For similar singularity models RUBBERT and SAARIS [16] for inlet flow and GILETTE [17] for nacelles have provided additional boundary conditions, prescribed in the fan plane. Yet, this approach leads to an increase in the leakage error. This error has been investigated for two different singularity models by SCHMIDT [18], figure 4.

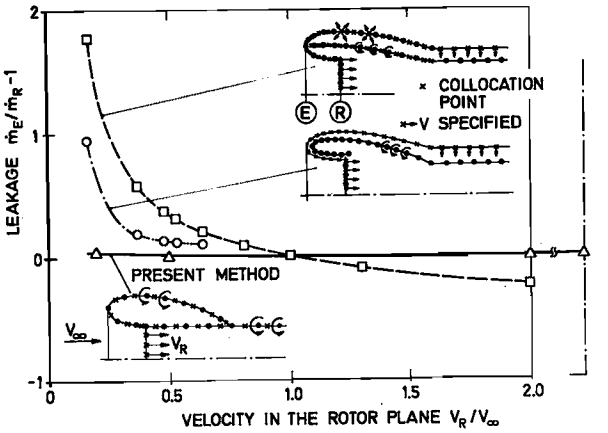

Figure 4. Leakage dependent on the mass flow ratio for different singularity models

Figure 4 shows the difference between the calculated mass flow rate and the prescribed mass flow rate in the rotor plane, depending on the onset flow ratio ("leakage"). Since the flow through the surface becomes maximal near to the rotor, figure 5, the application of an actuator disc turns out to be the main cause for the leakage increase. For this reason the application of such singularity planes was avoided when developing new mathematical methods, or the accuracy of the calculation was improved by suitable variation of the inlet geometry.

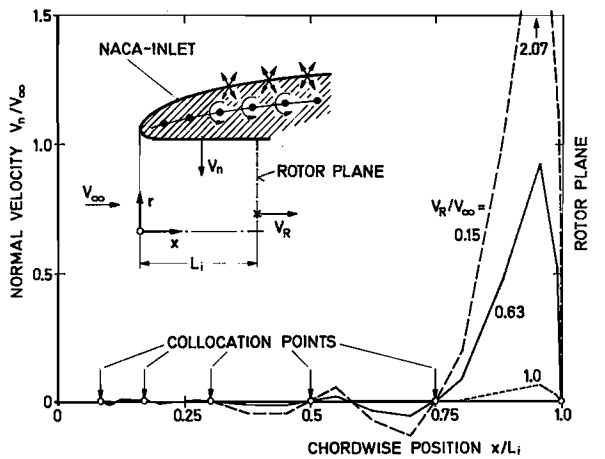

Figure 5. Computed leakage through the inner inlet surface (according to SCHMIDT [18])

In order to analyse the entire flow field around the engine, the entrainment velocities at the jet boundary as well as the inlet flow have to be known. The jet is considered to be a free jet with special initial conditions. The momentum is constant in longitudinal jet direction, the velocity distribution in a jet cross section remains affinitiv downstream the potential core region. Thus the velocity profiles in the fully developed turbulent jet region can be represented by a Gaussian distribution [19,20]. Because of the turbulent mixing at the jet boundary the environment air will

be accelerated in jet direction, jet mass flow and width increases, the maximum velocity decreases. Since no analytical solution of the turbulent flow mechanism in the jet exists, experimental results have to be used to develop a mathematical jet model. By integration of the known velocity profiles the jet mass flow can be determined at any jet cross section, so that the entrainment mass flow along the jet boundary and the corresponding velocities can be calculated [22,23]. In the non affinitiv region these velocities can be determined with empirical formulas according to SNEL [24]. For the calculation of the jet induced flow numerous singularity models have been developed which are using either line sinks along the jet axis, to generate entrainment flow [25], or sink- [24] or vortex sheet distributions at the surface [4].

Comparisons of theoretical and experimental results have shown [26,27] that a correct determination of the jet induced flow is only possible when not only the entrainment velocity at the jet boundary corresponds to the real physical conditions, but also the jet geometry. Considering jet cross-flow interference problems further developed models for the determination of the jet deflection and change in jet cross section have to be applied [28,29,30,31]. Also the interference with other bodies, ground effects and multi-jet interaction have a reasonable influence on the jet development, therefore an adaption of the boundary conditions to the geometrical situation becomes necessary [32].

4. CALCULATION OF THE ENGINE INDUCED FLOW FIELD

4.1 Adapted singularity model

Engine

According to the demonstrated state of art a mathematical model has been developed which enables the calculation of the engine induced flow in simultaneous consideration of inlet flow and turbulent jet entrainment. This model has the following properties:

- Leakage effects on the inlet contour are negligible for arbitrary onset flow conditions.
- An actuator disc is provided for controlling the mass flow rate.
- The entrainment velocities on the jet boundary can be prescribed as a function of the distance from the nozzle exit.

The exact reproduction of the physical flow by the mathematical one has been obtained in such a way that the engine contour also in a mathematical sense acts as a solid body and velocity discontinuities of the flow through the engine are avoided. For that reason the calculation model satisfies the following necessary and adequate conditions:

- The flow inside the fan shroud must vanish independent of the onset flow conditions.
- The continuity of the external and internal flow has to be preserved.

Hence, the corresponding singularity model follows immediately. The first condition can be satisfied only when vortices and doublets are used and arranged on the engine surface because the use of source sheets would induce a velocity jump perpendicular to the panel. Also for a flow through elements like an actuator disc or a jet boundary no source panel can be chosen because they would violate the continuity perpendicular to the panel. Only a non-lifting body like the center body is suited for using source panels because the resulting internal flow has no influence on the remaining flow field.

The resulting singularity distributions on the engine model are demonstrated in figure 6:

- Actuator disc with doublets,
- Fan shroud (engine contour) with vortices and near to the rotor plane additionally with doublets,
- Jet boundary with vortex sheets and with doublets,
- Center body with sources or sinks.

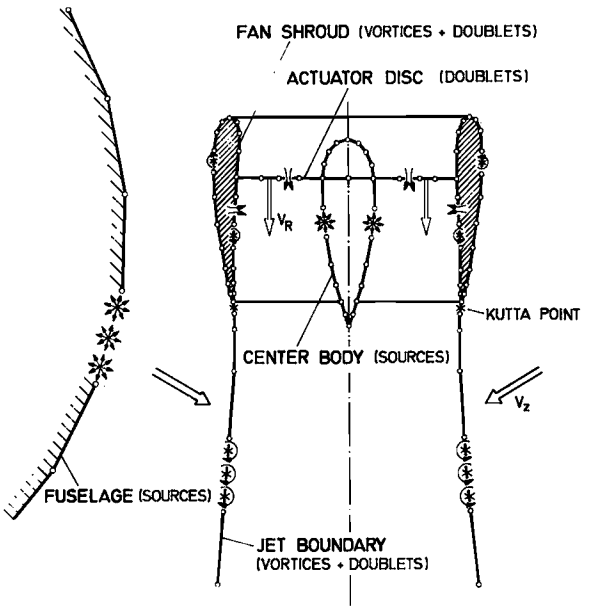

Figure 6. Singularity model of an engine airframe configuration

The intensity of the vortex sheet on the jet boundary is fixed by the vortex strength at the fan shroud trailing edge corresponding to a smooth flow over the trailing edge (satisfying the Kutta condition). This model can be superimposed with an arbitrary onset flow.

In order to exclude numerical problems arising as a result of distributing vortex sheets on the surface, on the other hand to use a physically meaningful boundary condition which in the first place influences the adjacent field of the singularity sheet, for the calculation of the vortex strength boundary conditions tangentially to the surface have to be used as an analogous approach to the source panel method. However, a flow normally through the panel can happen which cannot be neglected in particular when a strong cross flow exists. Such a cross flow arises by using an actuator disc in the end section of the inlet of the mathematical engine model: At the intersection of the rotor and the inlet contour a discrete vortex, as a

consequence of the doublet distribution on the rotor panels, yields a disturbance field on the engine contour normally to the adjacent surface, figure 7.

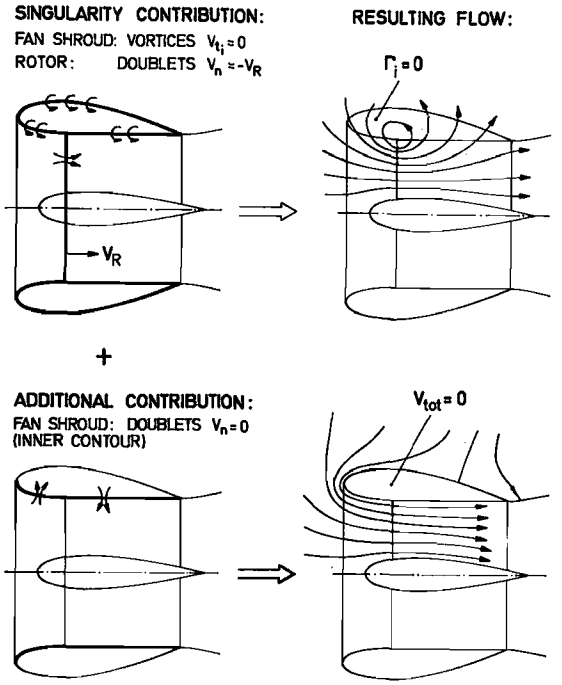

Figure 7. Schematic graph of the computed engine flow for different singularity models (static condition)

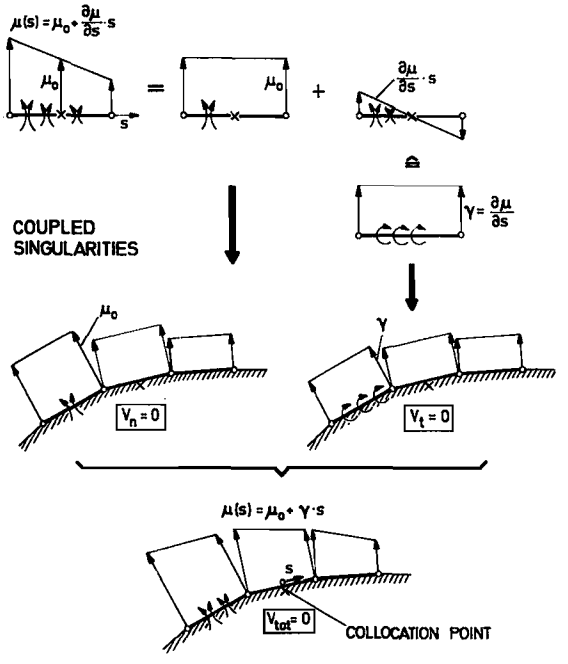

Figure 8. Superposition of singularities

The consequence is an increasing flow through the engine contour as demonstrated in figure 5. The suppression succeeds in a simple way by distributing additional doublet sheets on the engine surface. Their intensity is determined by the conventionally applied kinematic flow condition. Thereby it is sufficient to limit the doublet distribution to the inner part of the engine contour so that a cross flow cannot develop, figure 7. Thus in this region a distribution of vortex and doublet sheets and consequently a simultanous suppression of the velocity components normally and tangentially to the panel does exist. The total velocity in the collocation points of these panels, that is at $\bar{y} = -0$, therefore equals zero, figure 8. In this case it is inconsiderable whether the flow is twodimensional or axisymmetric.

Since in this paper the emphasis has been laid rather on an accurate engine model than on the jet model, as a first approach a simple law for the jet development [22] has been applied which in future efforts can be exchanged by a more sophisticated one.

Engine Wing Configuration

The described engine model can be combined with other bodies for the calculation of interference effects and secondary forces. In that case, the wing contour is generated by source distributions on the surface, and the Kutta condition is obtained from a vortex distribution, figure 9.

The model applied in the present calculations has been simplified to reduce computing time. It consists of an axisymmetric engine, coupled with a twodimensional unswept wing. This way, the change of the singularity intensities on the wing in spanwise direction as well as in the circumferential direction on the engine in fact have been neglected so that calculation errors can occur for small engine wing distances, but useful results are expected for conventional engine positions.

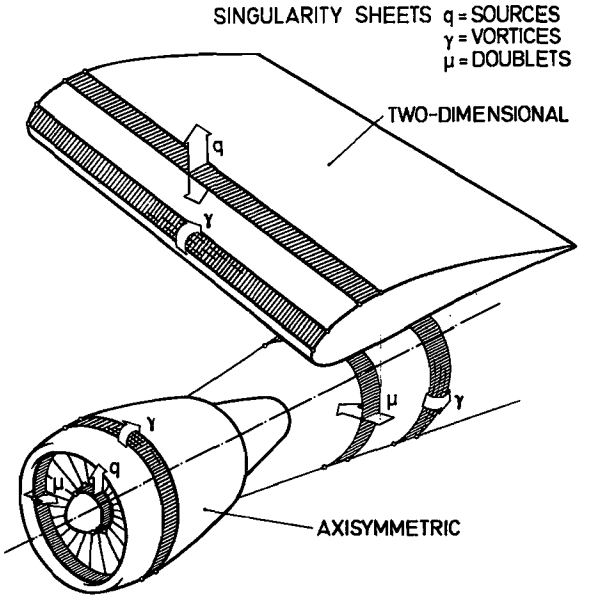

Figure 9. Mathematical model of an engine wing configuration

4.2 Boundary Conditions and Equation System

Boundary Conditions

The use of vortex distributions require some further consideration concerning the treatment of boundary conditions. Using the panel method in a way that sources and sinks are substituted by vortices, a plane panel does not induce a normal outward velocity component in its own collocation point, and the kinematic flow condition cannot be satisfied in the conventional application of $V_n=0$. The reason for this problem is the application of the conventional boundary condition which influences only the singularity intensities of the far field panels but not these of its own, although these intensities induce the major portion of the total velocity. Therefore numerical problems arise in the solution of the linear equations system, because all elements on the principal diagonal of the matrix of coefficients equal zero. Requiring instead a disappearing tangential velocity component on the panel, a predominant influence of the boundary condition on the near field portion of the induced velocity is caused. To obtain a vanishing flow inside the contour, the collocation point has to be defined on the lower side of the vortex panel. Thus the boundary condition with $\vec{t}$ as tangential unit vector yields

$$2\pi\,\gamma_i + \oint_A \frac{\partial}{\partial n}\left(\frac{1}{r_{i,j}}\right)\cdot\gamma_j\,dA = \vec{V}_\infty\cdot\vec{t} \qquad (5)$$

This equation is very similar to the kinematic flow condition equation (2).

In the case of zero onset flow the two boundary conditions differ only in the sign of the near field term resulting from the infinitesimally different position of the collocation points. For source panels the boundary condition is satisfied outside the contour (in the external flow), for vortex panels inside the contour (in the internal flow), figure 10.

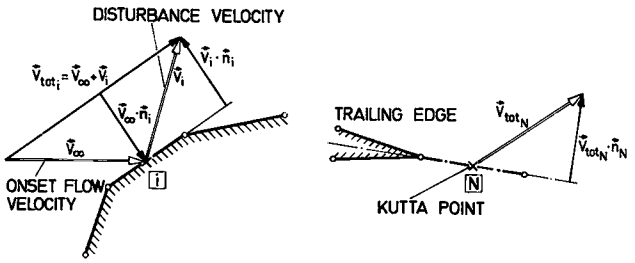

NORMAL VELOCITY COMPONENT = 0
(EXTERNAL FLOW):
$(\vec{V}_i + \vec{V}_\infty)\,\vec{n}_i = 0$

TANGENTIAL VELOCITY COMPONENT = 0
(INTERNAL FLOW):
$(\vec{V}_i + \vec{V}_\infty)\,\vec{t}_i = 0$

KUTTA CONDITION:

$\vec{V}_{tot_N}\cdot\vec{n}_N = 0$

Figure 10. Boundary conditions

Set of Linear Equations

The specified boundary conditions have to be satisfied in the collocation points of the panel model. By the discretization of the singularity model these boundary conditions lead to a linear equation system which, with the use of a source distribution for a replacement problem, yields

$$\sum_{j=1}^{N} a_{i,j}\cdot q_j = -\vec{V}_{\infty_i}\cdot\vec{n}_i\ , \qquad i = 1,\ldots N_1 \qquad (6)$$

In the collocation point i the normal components of the onset flow and the disturbance flow must be of the same magnitude and opposite direction. The disturbance velocity results from the summation of influences due to all source panels of intensity q_j. A coefficient of the equation system can be interpreted as a perpendicular component of the disturbance velocity to the panel i due to a source sheet of unit density on a panel j. For a constant source distribution on a 2D-panel, the velocity induction related to a panel coordinate system is

$$\vec{v}\,(x,y) = \left\{ \frac{1}{2}\ln\frac{x^2+y^2}{(x-\Delta s)^2+y^2}\ , \right.$$

$$\left. \arctan\frac{x}{y} - \arctan\frac{x-\Delta s}{y} \right\} \qquad (7)$$

From this equation a jump in the velocity distribution of 2π normal to the panel results for the collocation point in the middle of the panel

$$\vec{v}\left(\frac{\Delta s}{2}\ ,\pm 0\right) = \left\{0,\ \pm\pi\right\}$$

Thus the boundary condition has to be satisfied in the outside flow on the upper side of the panel. This restriction can be dropped by applying a doublet destribution. The disturbance velocity of a constant doublet sheet with unit intensiy ($\mu = 1$) yields

$$\vec{v}\,(x,y) = \Delta s\left\{ y\cdot\left(\frac{1}{(x-\Delta s)^2+y^2} - \frac{1}{x^2+y^2}\right)\ , \right.$$

$$\left. \frac{-(x-\Delta s)}{(x-\Delta s)^2+y^2} + \frac{x}{x^2+y^2} \right\} \qquad (8)$$

$$\vec{v}\left(\frac{\Delta s}{2}\ ,\ 0\right) = \left\{0,\ 4\right\}\ ,$$

and the flow through the panel in the collocation point is shown to be continous. Such a doublet panel is in particular suitable to define a flow through the surface by prescribing a specified velocity normal to the panel. In this case the boundary condition is

$$\sum_{j=1}^{N} a_{i,j}\cdot\mu_j = -\vec{V}_\infty\cdot\vec{n}_i + F_i\ , \qquad i = N_1 \ldots N_2 \qquad (9)$$

For the various parts of the contour with a doublet distribution one has to take the flow functions

- Inlet contour: $F_i = 0$
- Rotor plane: $F_i = -V_R$
- Jet boundary: $F_i = V_Z$

Thus a variation of the velocity ration V_R/V_∞ succeeds.

The flow fields of twodimensional source and vortex sheets of the equal geometry as well as of elemental sources and vortices are orthogonal.

Therefore the velocity induced by a vortex panel can be calculated with respect to equation (7). For the velocity components in the collocation point thus follows with $\gamma = 1$

$$\vec{v}\left(\frac{\Delta s}{2}, \pm 0\right) = \left\{\pm\pi, 0\right\}$$

The flow through the panel equals zero whereas the velocity in the panel direction shows a velocity jump of 2π. The application of the boundary condition in tangential direction, according to equation (5), results in

$$\sum_{j=1}^{N} b_{i,j} \cdot \gamma_j = -\vec{V}_{\infty_i} \cdot \vec{t}_i \quad , \qquad i = N_2 \ldots N_3 \quad . \quad (10)$$

In this case the influence coefficients are represented by the tangential component of the induced velocity due to all panels. Contrary to the kinematic flow condition for source panels from equation (6), equation (10) has to be satisfied for inside flow.

The total set of equations can be derived by application of the three boundary conditions equation (6), (9) and (10) for the different singularity distributions of the panel model. As an example, the coefficient matrix of such an equation system for a symmetric engine contour is shown in figure 11. This scheme is valid for the twodimensional as well as for the axisymmetric flow but the value of the coefficients differ according to the chosen case.

SINGULARITIES:

COLLOCATION POINTS:	VORTICES	DOUBLETS		SOURCES	
	INFLUENCE OF				
TANGENTIAL COMPONENTS	FAN SHROUD VORTICES ON ENGINE CONTOUR	FAN SHROUD DOUBLETS ON ENGINE CONTOUR	JET DOUBLETS ON ENGINE CONTOUR	ROTOR DOUBLETS ON ENGINE CONTOUR	CENTER BODY SOURCES ON ENGINE CONTOUR
NORMAL COMPONENTS	FAN SHROUD VORTICES ON ENGINE CONTOUR	FAN SHROUD DOUBLETS ON ENGINE CONTOUR	JET DOUBLETS ON ENGINE CONTOUR	ROTOR DOUBLETS ON ENGINE CONTOUR	CENTER BODY SOURCES ON ENGINE CONTOUR
	FAN SHROUD VORTICES ON JET	FAN SHROUD DOUBLETS ON JET	JET DOUBLETS ON JET	ROTOR DOUBLETS ON JET	CENTER BODY SOURCES ON JET
	FAN SHROUD VORTICES ON ROTOR	FAN SHROUD DOUBLETS ON ROTOR	JET DOUBLETS ON ROTOR	ROTOR DOUBLETS ON ROTOR	CENTER BODY SOURCES ON ROTOR
	FAN SHROUD VORTICES ON CENTER BODY	FAN SHROUD DOUBLETS ON CENTER BODY	JET DOUBLETS ON CENTER BODY	ROTOR DOUBLETS ON CENTER BODY	CENTER BODY SOURCES ON CENTER BODY

Figure 11. Physical interpretation of the influence coefficients (symmetric engine singularity model)

Figure 11 also contains the equation system for a combination of an engine and a wing. In this case the calculation of the influence coefficients is obtained in the following way:

- matrix "engine" corresponding to figure 11 with the relevant formulas for axisymmetric flow (33)
- matrix "wing" with equation (7) for source and vortex panels at two-dimensional flow
- interference matrix "E" - "W" with relevant formulas for axisymmetric flow (33) and determination of the normal component according to figure 12
- interference matrix "W" - "E" with equation (7) for two-dimensional flow.

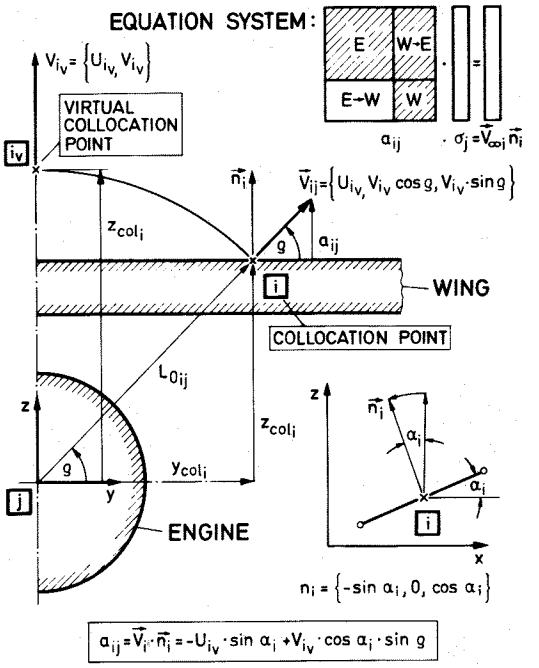

Figure 12. Wing panel influence coefficients

The consideration of the wake is not necessary, because the variation of the singularity intensities in spanwise direction of the wing has been neglected.

4.2 Pressure distribution

The solution of the linear equation system can for example be performed with Gauß algorithm. It delivers the intensities of the source, vortex and doublet singularities which generate the desired contour of the body. With this solution, the total velocity can be determined at any point of the flow field by summation of the onset flow and the disturbance velocities of all panels.

$$\vec{V}_{tot_i} = \sum_{j=1}^{N} \vec{V}_{ij} \cdot \sigma_j + \vec{V}_{\infty_i} \quad , \qquad i = 1, \ldots N$$

Here, σ_j is the intensity of the singularity of the panel j. The velocity at the control points of the vortex panels of the engine contour can be obtained immediately from the vortex strength with

$$\vec{V}_{tot_i} = 2\pi \gamma_i$$

since all singularities are calculated such that within the engine contour the total velocity disappears. Then the corresponding pressure coefficient for incompressible flow is

$$c_{p_i} = 1 - \left(\frac{V_{tot_i}}{V_{\infty_i}}\right)^2 \quad .$$

5. COMPUTATIONAL RESULTS

5.1 Singular Engines

To check the quality of the developed computational method for axisymmetric engines, the flow field has been calculated for chosen engine contours at different onset flow velocities.

As a first engine contour a modified NACA 0018 annular wing has been used with such a camber that from the point of maximum thickness the aftend of the inner surface is a cylinder. A center body has been placed to simulate a real inflow. Figure 13 shows the calculated velocity field for the static condition:

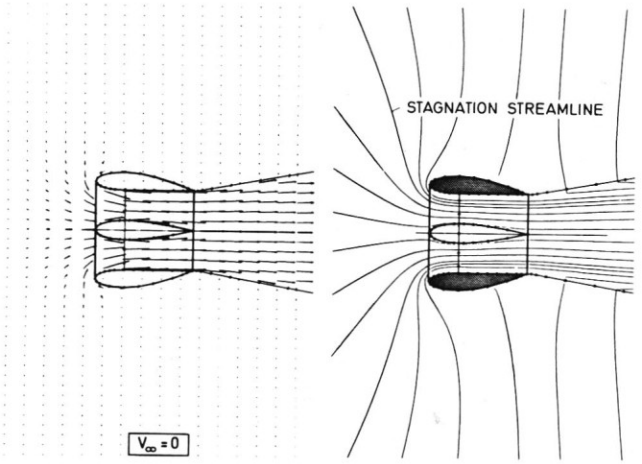

Figure 13. Velocity field and streamlines, computed for axisymmetric flow (static condition)

The velocity vectors of the flow field show that the engine inlet flow dominates the flow towards the jet. The induced velocities very quickly decrease with increasing distance from the engine. In a distance of about one engine diameter from the inlet respective the jet, the induced velocities are close to zero. The velocities induced inside the center body are not included in the picture, because this internal flow has no physical meaning and is without significance for the rest of the engine flow. On the other hand, the induced velocities within the engine contour have been calculated at various points. As the picture shows, there is no inside flow. In consequence of that, in the outside flow in the immediate vicinity of panel boundaries, the velocity is tangential to the surface although the collocation points are in some distance. That indicates that the developed panel model very well satisfies the requirement of preventing a flow perpendicular to the surface.

To demonstrate the continuity of the flow, a stream line picture has been calculated and added in figure 13. It is remarkable that in all areas the flow is continous especially through the rotor plane which shows that the application of doublet panels in this area is correct. In addition, the stagnation streamline has been calculated which divides the flow into the inlet flow and the flow towards the jet. This line ends in the stagnation point which in this case - zero onset flow velocity - is located in 65 per cent of the chord length.

The streamlines for an onset flow velocity ratio $V_\infty / V_R = 0{,}25$ shows the same quality of the developed mathematical model, figure 14.

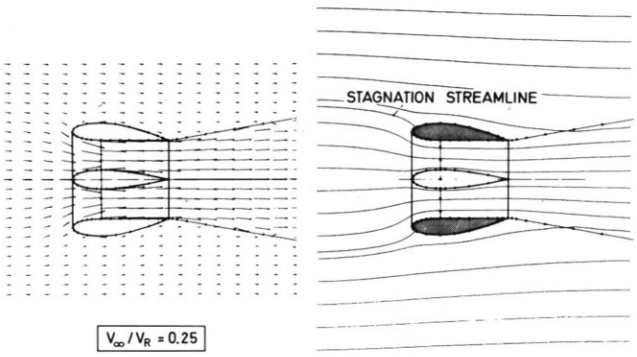

Figure 14. Velocity field and streamlines for axisymmetric flow (flight condition)

Again the flow is continous and the induced velocities within the engine contour are close to zero. The stagnation point in this case has moved foreward to the leading edge of the inlet corresponding to take off conditions of aircraft. Caused by the fast decrease of the engine induction, undisturbed parallel flow exists already in a lateral distance of only one engine diameter.

To verify the computational results, experiments have been performed for an engine model at static condition. This engine model is designed as an ejector engine. The jet is generated with pressurized air which is ejected in the rotor plane so that at the same time the inlet flow and the jet can be simulated, figure 15. The curvature of the engine shroud corresponds to the calculated modified NACA 0018 profile, the ratio of the diameters of center body and shroud is $d_i/d_e = 0{,}53$.

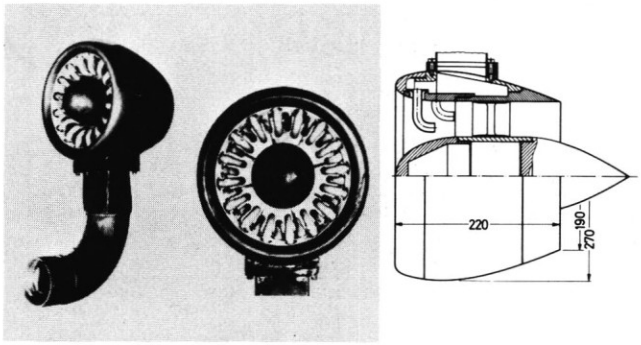

Figure 15. Ejector engine with pressure air duct

For computation of the axisymmetric flow around this engine the mathematical model has been slightly adapted to the experimental model: the increased mass flow due to the additional pressurized air has been taken into account. The results are shown in figure 16. The focus in this picture is in the flow inside the engine, and for this reason a larger scale has been selected. One can recognize that a strong contraction of the flow at the inlet takes place and that within the engine contour the flow disappears and the velocity vectors are reduced to points.

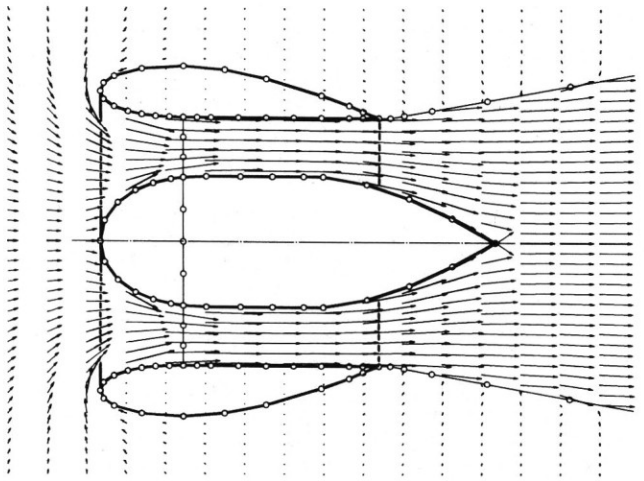

Figure 16. Computed flow field of an axisymmetric ejector engine model (static condition)

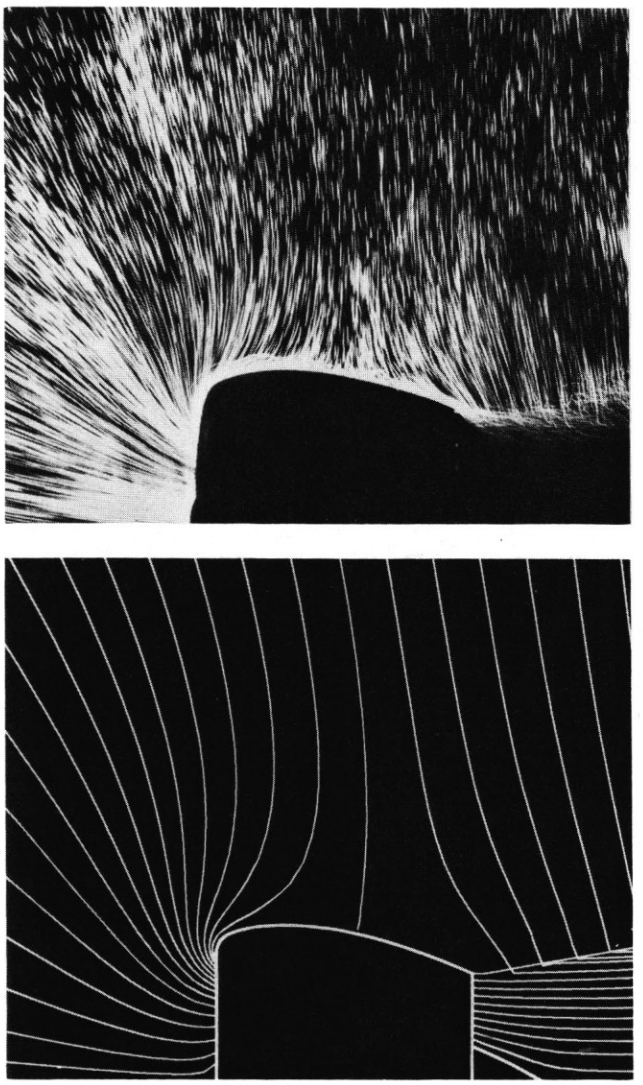

Figure 17. Comparison of experimental and computational flow field at the ejector engine

In Figure 17 this flow field is compared to an experimental one. The photograph on the upper half has been taken according to the light section method (33). In this method only one plane of the complete flow field is illuminated. The air around the model engine contains white, strongly reflecting polyaethylen particles which are illuminated by the light section and can be photographed against the dark background. With a time exposure the particles appear as streaks which are parallel to the stream lines. The light section has been put through the center line. The lower half of figure 17 also shows the streamlines calculated according to the panel model of figure 16. The coincidence of the experimental flow field and the computed one is very good in all areas. Even the stagnation point has an identical position in both pictures.

Within an engine inlet strong interferences can occur. This is shown for the static condition in figure 18. It shows the relative velocity on the ejector shroud for different center bodies. The influence of the center body on the flow around the leading edge of the engine is obvious. With increasing diameter of the center body the velocities at the inlet contour decrease due to the contraction of the inlet flow. Therefore the form of the center body can have a considerable influence on the design of the engine inlet.

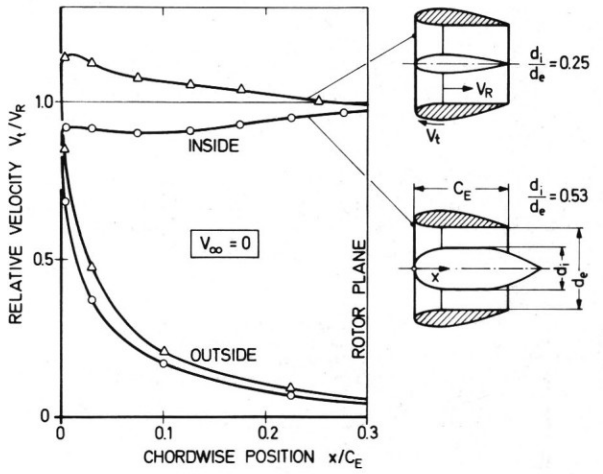

Figure 18. Computed velocities at a NACA 0018 inlet for different center bodies

For a further check of the computational method the pressure distribution of an axisymmetric inlet has been calculated for two different mass flow ratios and compared with measurements of NASA (34). Here, contrary to the previously investigated engine inlets, a relatively thin annular wing section NACA 1-85-100 with a keen leading edge ($r/D_{max} = 0.0018$) has been used. The onset flow velocity is of the same order as the velocity in the entrance plane. Figure 19 shows the results. For both mass flow ratios the measured and the calculated pressures coincide to a large extend. A significant difference of experiment and calculation is only found at a mass flow ratio of $\dot{m}/\dot{m}_\infty = 1.16$ at the inner part of the inlet. This difference can be traced back to viscous effects. The steep pressure rise leads to a quick increase of the

boundary layer thickness which changes the effective inlet contour so that the real flow decelerates less than the computed potential flow.

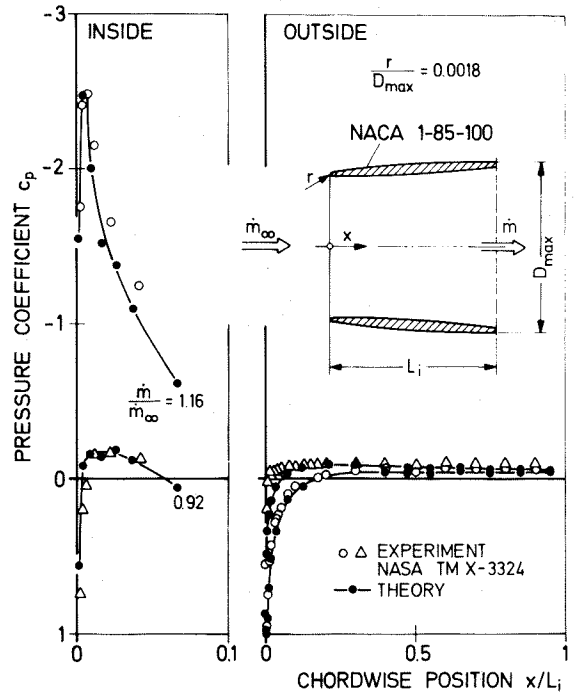

Figure 19. Pressure distribution at an axisymmetric inlet NACA 1-85-100 for different mass flow rates

Another example is calculated in order to compare the results of the present method with other computational methods, especially higher order panel methods. The results are shown in figure 20:

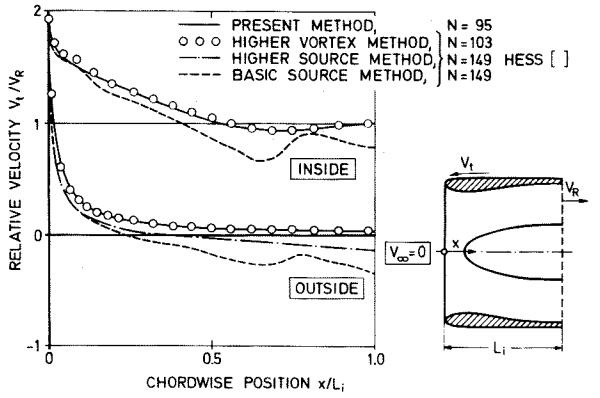

Figure 20. Computed surface velocities at an axisymmetric inlet

For the inlet flow there is a very good agreement with a higher order vortex panel method according to HESS and MARTIN (5) which can be considered as a very accurate solution because control calculations with the double number of panels have shown no improvement. Computational methods which apply only source panels are less accurate. Even a higher order source panel method with a higher number of panels renders correct velocities only inside of the inlet. Outside of the shroud results a non realistic direction of the flow which is indicated by an additional stagnation point. The basic method, applying source panels with constant strength on the surface only, yields results with considerable errors all over the engine contour.

This shows that the presented computational method, which can be described as a modified panel method with a combination of vortex and doublet panels, is superior even to higher order source panel methods. It has an accuracy which compares well with a higher order vortex panel method although the theory is as uncomplicated as the basic method. Furthermore, it seems that there are no constraints to be considered concerning the geometry of the engine and the onset flow conditions. The method enables the theoretical treatment of the aerodynamic properties of engine inlets and nacelles for the entire flight speed range.

Therefore the computational method has been applied to a more realistic engine geometry. The results are shown in figure 21 for three different flight speeds. As in the former examples, the velocity inside the engine contour equals zero (left part). The right part shows the corresponding streamlines.

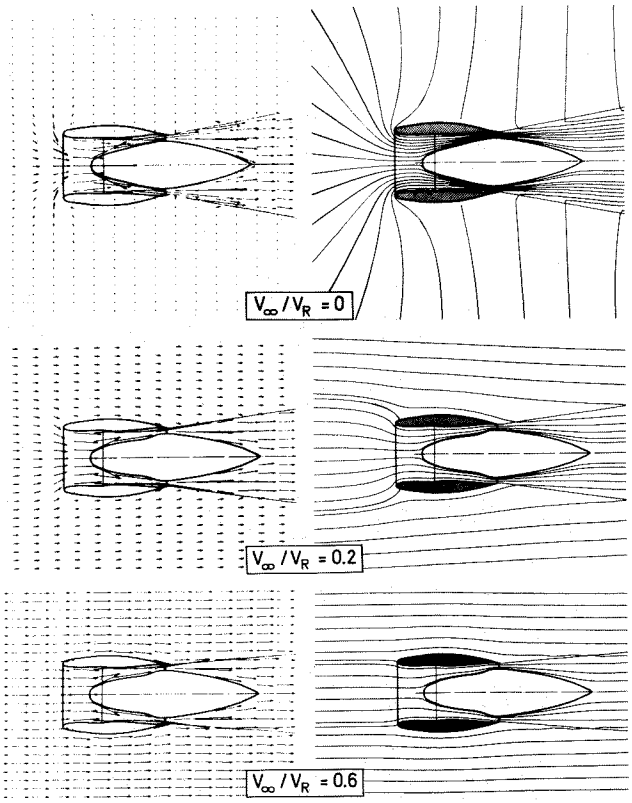

Figure 21. Computed flow field for different onset flow velocities

Figure 22 shows the velocities on the surface and the resulting pressure distributions. On the major part of the inner side of the inlet nearly a constant pressure is obtained for any flight speed. On the other hand, on the outer contour of the engine shroud the pressure gradient along the surface

is negative for low flight speeds and positive for high flight speeds. Furthermore it seems remarkable that a negative pressure peak is observed at the leading edge of the inlet only at very low or very high flight speeds. For $V_\infty / V_R = 0.4$ this negative pressure peak is on the inner side, at $V_\infty / V_R = 1$ it is found on the outer side of the inlet. For $V_\infty / V_R = 1$ a compressibility correction according to Krahn has been applied.

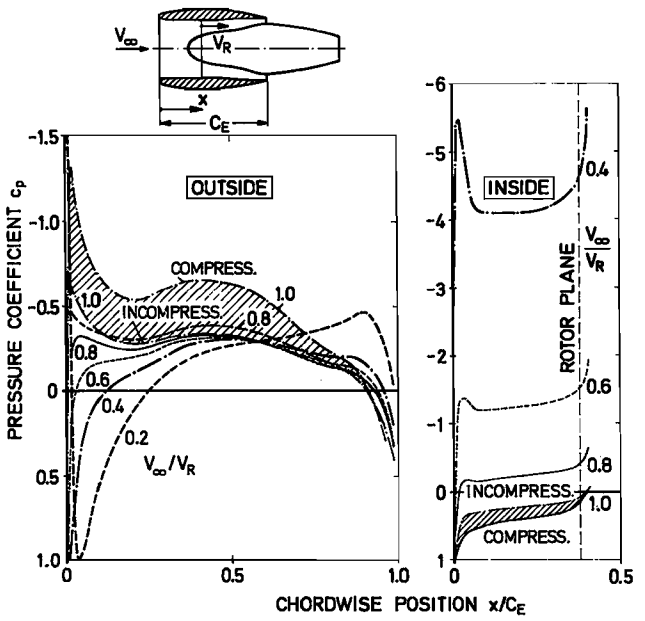

Figure 22. Influence of onset flow velocities on the pressure distribution at the engine

5.2 Engine Wing Configuration

In extension of the calculations the engine has been combined with a cambered wing section with rear loading (infinite unswept wing). For an onset flow velocity $V_\infty/V_R = 1$ and a specified vertical and chordwise engine position the spanwise pressure distributions have been calculated in figure 23.

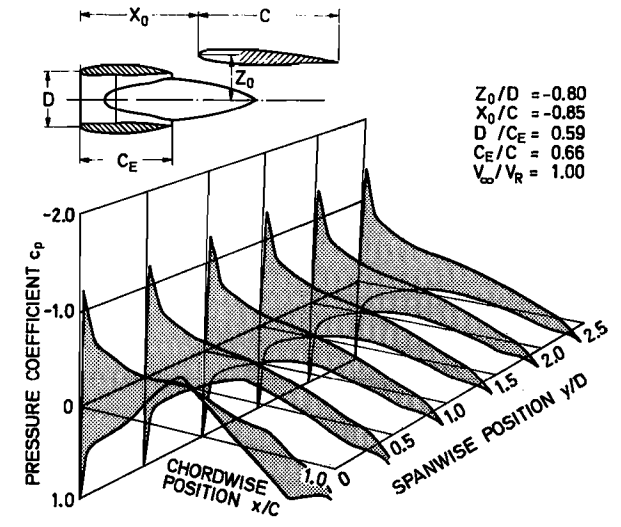

Figure 23. Pressure distribution on an infinite wing (engine below the wing)

It shows that the influence of the inlet flow is very limited in spanwise direction. In a distance of only two engine diameters the influence is already negligible. The main interference influence is found on the lower side of the airfoil where at engine position (y/D = 0) a negative pressure coefficient difference between upper and lower side is obvious.

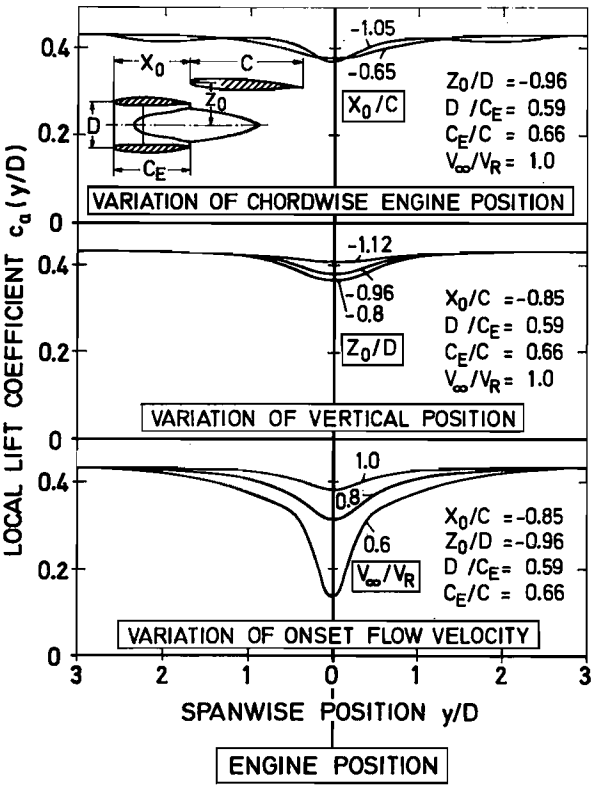

Figure 24. Local lift coefficient on an infinite wing dependent on chordwise and spanwise engine position and onset flow velocity

The results of a parametric variation of the onset flow velocity and the engine position relative to the wing (33) are summarized in figure 24:

- The variation of the onset flow velocity shows a significant difference in the local lift coefficient at low or high flight speeds. At low speed a considerable interference is noticable. The local lift coefficient in the vicinity of the engine is greatly decreased which is caused by the increased entrainment flow to the jet. This leads to a decrease of the negative pressure peak at the leading edge of the wing and a negative pressure difference at approximately the middle of the chord at y/D = 0.
- As it is to expect the influence of interference is decreased when the engine is at a larger vertical distance of the wing. However, if the engine is mounted very closely to the wing (figure 23), the flow on the upper airfoil side is nearly without influence, even close to the leading edge.
- If the chordwise position is varied, a flow interference at the leading edge is very noticable. If the trailing edge of the engine and the lead-

ing edge of the wing are just positioned one above the other, the flow around the leading edge of the wing is restrained resulting in a smaller lift coefficient. When the engine is mounted more foreward the interference concerns only the lower side of the airfoil, leading to a more spanwise influence on the lift coefficient.

Additionally, pressure distributions for engines mounted above the wing have been performed (33). As an example, for $V_\infty/V_R = 1$ and specific engine positions the spanwise pressure distributions are shown in figure 25.

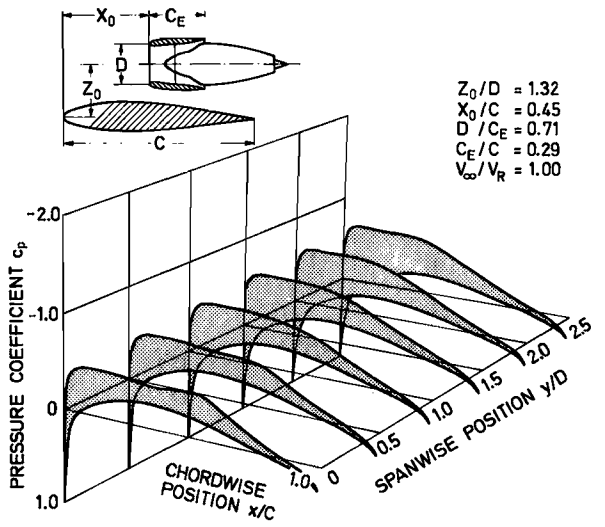

Figure 25. Pressure distribution on an infinite wing (engine above the wing)

In this example a very small engine wing distance has been chosen leading to a lift decrease which results from a pressure drop on the upper side of the wing ahead of the engine intake.

5.3 Leakage Effects

For an estimation of the leakage effect which may cause an error in the developed computational model the two-dimensional flow around a single engine has been investigated. The results, as a consequence of the stronger replacement effect, are also representative for the axisymmetric case. The continuity of the flow has been investigated in the engine inlet control area which is bordered by the entrance plane, the inner inlet contour, the rotor plane and the center body. On account of symmetry the flow has been considered only on one side of the engine axis. The difference in mass flow rate, entering the control volume through the entrance plane and leaving it through the rotor plane, corresponds to the leakage flow which leaves the control area through the engine shroud surface.

Figure 26 shows the calculated distributions of the velocities perpendicular to the entrance plane and rotor plane respectively for different onset flow velocities. For all velocity profiles a mean velocity of $\bar{V}_R = 1$ is obtained in the actuator disc. For reasons of continuity, corresponding to the ratio of rotor plane area and entrance plan area, the mean velocity in the entrance plane for the selected geometry has to be $\bar{V}_E = 0.6$. This value can be verified by means of the calculated velocity distributions in figure 26.

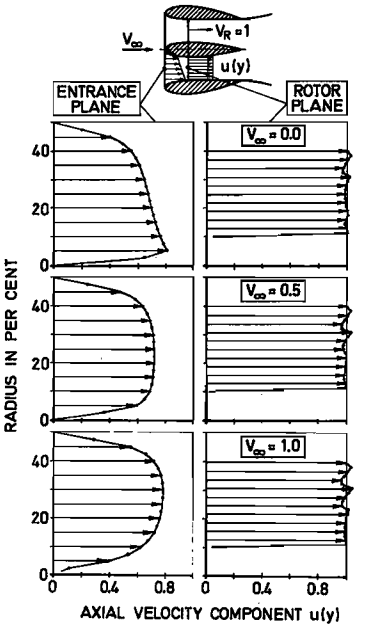

Figure 26. Velocity distribution in the engine inlet dependent on the onset flow velocity

A numerical integration has been performed for a range of onset flow velocities of $0 \leq V_\infty/V_R \leq 5$, resulting in a maximal error of 3,6 per cent, figure 4. That means that in the applied singularity model calculation errors due to leakage through the engine contour are negligible for all practical flight speeds.

6. CONCLUDING REMARKS

Based on the concept of an adapted singularity model the present panel method for the axisymmetric engine appears to be capable to provide reasonable results. However, real flow around engine wing configurations requires an extension of the theory in order to get the method more general for an application to design optimization. Therefore future efforts for the following subjects will be necessary:

- The axisymmetric engine model should be extended to a three-dimensional one to allow non axisymmetric flow (engine at angle of attack, multi-engine configuration) and geometry (optimization of the engine contour due to the wing influence on the engine).
- In order to adapt the exhaust jet model to that of a high bypass engine with a fan jet contraction along the afterbody, a parametric treatment of the jet characteristics appears desirable, especially for the purpose of using experimental results.
- The extended engine model should be coupled with an existing three-dimensional wing panel method to include modern wing and pylon design.
- Finally it appears necessary to check the theoretical results with existing wind tunnel mea-

surements and with turbo power simulation tests.

7. REFERENCES

(1) Hess,J.L. and Smith,A.M.O.: "Calculation of potential flow about arbitrary bodies". Progress in Aeronautical Sciences, Vol. 8, Pergamon Press, London, New York, Paris, 1967.

(2) Kraus,W. and Sacher,P.: "Das MBB-Unterschall-Panelverfahren". Teil 1-3, MBB-UFE 632-70 bis 634-70, 1970.

(3) Schmidt,W.: "Potentialtheoretische Berechnungsverfahren für Unter- und Überschallströmungen. Ein kritischer Überblick". Bericht 74/54, Dornier GmbH, Friedrichshafen.

(4) Johnson,F.T. and Rubbert,P.E.: "Advanced panel-type influence coefficient methods applied to subsonic flows". AIAA Paper 75-50.

(5) Hess,J.L. and Martin,R.P.: "Improved solution for potential flow about arbitrary axisymmetric bodies by the use of a higher-order surface source method". NASA CR 134694, July 1974.

(6) Rubbert,P.E. and Saaris,G.R.: "A general three-dimensional potential-flow method applied to V/STOL aerodynamics". SAE Paper 680304, 1968.

(7) Kraus,W. and Sacher,P.: "Das Panelverfahren zur Berechnung der Druckverteilung von Flugkörpern im Unterschallbereich". ZfW 1973, Heft 9.

(8) Hess,J.L.: "Higher order numerical solution of the integral equation for the two-dimensional Neumann problem". Computer methods in applied mechanics and engineering 2 (1973).

(9) Hunt,B. and Semple,W.G.: "Economic improvements to the mathematical model in a plane/constant-strength panel method". Euromech colloquium 75, Rhode May 1976.

(10) Küchemann,D. and Weber,J.: "Aerodynamics of propulsion". McGraw-Hill, New York, Toronto, London, 1953.

(11) Hess,J.L. and Smith,A.M.O.: "A general method for calculating low speed flow about inlets". AGARDograph 103, pt.1, 1965.

(12) Zimmer,H.: "Berechnung der Druckverteilung an dreidimensionalen Unterschall-Triebwerkseinläufen mit dem Quellpanel-Verfahren". Dornier AG, Friedrichshafen, Vortrag vor dem DGLR-Fachausschuß für luftatmende Antriebe, Friedrichshafen, Dez. 1972.

(13) Stockman,N.O.: "Potential and viscous flow in VTOL, STOL or CTOL propulsion system inlets". AIAA Paper No. 75-1186.

(14) Geißler,W.: "Berechnung der Potentialströmung um rotationssymmetrische Ringprofile". ZfW 1973, Heft 1.

(15) Trulin,D.J. and Iversen,J.D.: "Pressure distribution about a finite axisymmetric nacelle". J. Aircraft 1970, No. 1.

(16) Rubbert,P.E. and Saaris,G.R.: "Review and evaluation of a three-dimensional lifting potential flow analysis method for arbitrary configurations". AIAA Paper No. 72-188.

(17) Gilette,W.B.: "Nacelle installation analysis for subsonic transport aircraft". AIAA Paper No. 77-102

(18) Schmidt,W.: "Aerodynamic influence coefficient methods for subsonic and supersonic potential flow - a critical survey". Euromech Colloquium 75, Rhode May 1976.

(19) Reichardt,H.: "Gesetzmäßigkeiten der freien Turbulenz". VDI-Forschungsheft 414 (1942), 2. Aufl. Düsseldorf 1951.

(20) Biringen,S.: "The prediction of an axisymmetric turbulent jet by a three-equation model of turbulence". VKI-TN 114, 1975.

(21) Schlünder,E.U.: "Über die Ausbreitung turbulenter Freistrahlen". ZfW 1971, Heft 3.

(22) Liem,K.: "Strömungsvorgänge beim freien Hubstrahler". Luftfahrttechnik 8 (1962) Nr. 8.

(23) Seibold,W.: "Untersuchung über die von Hubstrahlen an Senkrechtstartern erzeugten Sekundärkräfte". Jahrbuch der WGLR 1962.

(24) Snel,H.: "A method for the calculation of the flow field induced by a free jet". NLR TR 72040 U.

(25) Kraemer,K.: "Die Potentialströmung in der Umgebung von Freistrahlen". ZfW 1971, Heft 3.

(26) Barche,J.: "VSTOL aircraft prediction methods. Part 1: Jet interaction out of ground effect (OGE)". VFW Kurzbericht Ef - 526/1, 1975.

(27) Siclari,M.J., Barche,J. and Migdal,D.: V/STOL aircraft prediction technique development for jet-induced effects". Naval Air Propulsion Test Center, Trenton, N.J., GACPDR-623-18 (1975).

(28) Wooler,P.T.: "On the flow past a circular jet exhausting at right angles from a flat plate or wing". The Aeronautical Journal, March 1967.

(29) Skifstad,J.G.: "Aerodynamics of jets pertinent to VTOL aircraft". J. Aircraft 1970, No. 3.

(30) Snel,H.: "A potential flow model for the flow field induced by a jet exhausting into a uniform cross flow". NLR TR 73048 U.

(31) Schmitt,H.: "Änderung einer Parallelströmung entlang einer ebenen Platte durch einen quer gerichteten Freistrahl". ZfW 1979, Heft 5.

(32) Strauber,M.: "Berechnung von Strahlkonturen mit Hilfe eines Wirbelringmodells". ZfW 1975, Heft 11.

(33) Göde,E. and Haberland,C.: "Berechnung des Strömungsfeldes um Triebwerk-Flügel-Konfigurationen". ILR-Bericht 43 (1979), Institut für Luft- und Raumfahrt, TU Berlin.

(34) Hertel,H. and Harmsen,S.: "Wandströmungen und Aufströme aus der Umlenkung von Freistrahlgruppen". VDI-Fortschr.-Ber. Reihe 12, Nr. 11, 1966.

(35) Re,R.J.: "An investigation of several NACA 1-series inlets at Mach numbers from 0.4 to 1.29 for mass-flow ratios near 1.0". NASA TM X-3324, 1975.